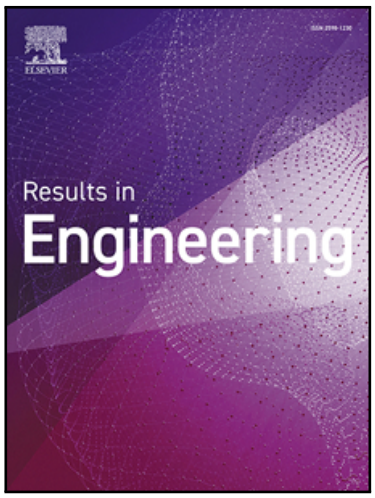

Fabrication of a microheater based on silver-polyimide metallization with enhanced thermal and mechanical stability

Deni Haryadi , Jos Istiyanto , Bambang Suryawan , Azizah Intan Pangesty , Sugeng Supriadi , Jerome Charmet , Yudan Whulanza

PII: S2590-1230(25)00546-8
DOI: https://doi.org/10.1016/j.rineng.2025.104468
Reference: RINENG 104468

To appear in: *Results in Engineering*

Received date: 24 December 2024
Revised date: 19 February 2025
Accepted date: 23 February 2025

Please cite this article as: Deni Haryadi , Jos Istiyanto , Bambang Suryawan , Azizah Intan Pangesty , Sugeng Supriadi , Jerome Charmet , Yudan Whulanza , Fabrication of a microheater based on silver-polyimide metallization with enhanced thermal and mechanical stability, *Results in Engineering* (2025), doi: https://doi.org/10.1016/j.rineng.2025.104468

Highlights

- A flexible silver-PVA microheater was fabricated, achieving a rapid heating response up to 160°C at 1.50 V, with a stable temperature over extended periods.
- Using an innovative combination of surface modification ion exchange (SMIE) and doctor blade deposition, the patterned heating electrode (293–2998 µm wide, 28 µm thick) demonstrated superior adhesion and enhanced stability.
- The SMIE method significantly improved adhesion, thermal stability (TGA shows decomposition temperature up to 620°C), and mechanical reliability (maintaining resistance with <1% change after 5000 bending cycles).
- SEM and EDS analyses revealed a highly uniform distribution of silver particles, reducing porosity at higher voltages, leading to enhanced electrical and thermal conductivity.
- The developed microheater presents a cost-effective, scalable, and adaptable solution for disposable and flexible biomedical and electronic applications.

Fabrication of a microheater based on silver-polyimide metallization with enhanced thermal and mechanical stability

Deni Haryadi [1,2], Jos Istiyanto [1], Bambang Suryawan [1,2], Azizah Intan Pangesty[3,4], Sugeng Supriadi[1,4], Jerome Charmet [5,6*], Yudan Whulanza [1,4*]

[1]Department of Mechanical Engineering, Faculty of Engineering, Universitas Indonesia, Depok 16424, Indonesia
[2] Department of Mechanical Engineering, Gunadarma University, Depok 16424, Indonesia
[3]Department of Metallurgical and Materials Engineering, Faculty of Engineering, Universitas Indonesia, Depok 16424, Indonesia
[4]Research Center for Biomedical Engineering, Universitas Indonesia, Depok 16424, Indonesia
[5]School of Engineering HE-Arc Ingénierie, HES-SO University of Applied Sciences Western Switzerland, 2000 Neuchâtel, Switzerland
[6]Faculty of Medicine, University of Bern, 3010, Bern, Switzerland

yudan.whulanza@ui.ac.id

Abstract

The development of flexible, reliable, and cost-effective microheaters is critical for applications requiring precise thermal management. This study presents a novel approach for fabricating flexible silver microheaters using a solution-based polyimide metallization process. By integrating the surface modification ion exchange (SMIE) method with electronic craft cutting, we enhanced electrode adhesion and achieved consistent pattern quality, making the fabrication process more accessible and scalable. The heaters demonstrated excellent thermal properties with a high decomposition temperature of 620°C and enhanced thermal stability. Thermal characterization using thermogravimetric analysis and differential scanning calorimetry confirmed improved stability, whereas heating performance evaluation showed consistent temperature regulation. The heating performance tests showed rapid temperature increases, achieving approximately 160°C at 1.50 V and stable temperatures maintained for 60 min under continuous operation. Elemental composition and surface morphology analyses revealed a uniform distribution of silver particles and decreased porosity at higher voltages, enhancing electrical and thermal conductivity. X-ray Diffraction analysis confirmed increased crystallinity at higher voltages, which was correlated with improved material quality. The mechanical durability tests indicated that the heaters could withstand over 5000 bending cycles without significant performance degradation, confirming their robustness for flexible applications. This approach presents a scalable, low-cost alternative to traditional microheater fabrication, opening new opportunities in wearable electronics and point-of-care diagnostics.

Keywords: flexible microheaters; polyimide metallization; surface modification ion exchange.

1. INTRODUCTION

The integration of microheaters into modern microfluidic devices enables precise temperature control in small, confined spaces—crucial for applications such as detectors, sensors, thermal therapy, and tumor ablation (Andreozzi et al., 2022; Gu et al., 2021; Irwansyah et al., 2021; Li et al., 2022; Lischer et al., 2021). In life science-on-chip applications, micro heating modules play an essential role in tasks like culturing cells (Whulanza et al., 2014), drug delivery (Nadhif et al., 2017), droplet encapsulation (Whulanza et al., 2023), and DNA extraction (Josephin et al., 2024). Additionally, precise temperature control is indispensable for accurate nucleic acid amplification testing (NAAT), making reliable microheaters a key component in these devices (Kitagawa et al., 2020; Roberts et al., 2021; Y. Zhang et al. (2020).

Traditionally, microheater fabrication relied on classic microfabrication techniques such as photolithography and thin-film deposition of metals such as platinum, copper, and titanium onto polymeric substrates. While these methods yield high-performance microheaters, they are often time-consuming, costly, and require specialized cleanroom environments, limiting their scalability and accessibility (Al-Mohsin et al., 2022; Charmet et al., 2020). The high production costs and complexity make it difficult to scale up conventional microheaters for mass production.

Recently, there has been a shift toward more accessible fabrication methods, such as printing techniques and mechanical patterning. These new approaches aim to democratize microheater production by reducing the need for specialized infrastructure, thus making the fabrication process more cost-effective, adaptable, and scalable (Solangi et al., 2024). Despite these advancements, challenges remain—particularly concerning the durability of microheaters under extreme conditions, such as repeated thermal cycling or long-term use, which can lead to performance degradation or device failure (Barman et al., 2018; Byers et al., 2020; Qaiser et al., 2023; Wang et al., 2019). A significant issue here is the mismatch between the thermal expansion coefficients of the microheater and the polymeric substrate, which generates shear stress during heating cycles. This stress can cause delamination and breakage of the microheater (Aleksandrova et al., 2024; Yan et al., 2017). Additionally, the lack of flexibility in the microheaters of many existing microfluidic devices complicates their integration into miniaturized devices (B. Lee et al., 2023; Wang et al. (2019).

To address these issues, the improvement of adhesion between the metal electrodes and the polymeric substrate through polymeric metallization was explored. The surface modification ion exchange (SMIE) method, which enhances adhesion by exchanging the surface atoms of the polymeric substrate with those of the deposited metal, has shown promise. However, the resulting electrodes often lacked the desired thermal stability (Hou & Zhang, 2018; N. Zhang, Huang, Wan, Kang, et al., 2019; Q. Zhang et al. (2023).

In this study, we address these reliability challenges by integrating a silver nanocomposite with the SMIE method. This approach, combined with polyimide metallization, not only improves electrode adhesion and ensures consistent pattern quality, making it an ideal solution for developing flexible microheaters. The resulting nanocomposite microheater exhibits precise temperature control and maintains stability during long-term use and thermal cycling even after repeated bending. Additionally, we introduce the use of electronic craft cutters for electrode patterning, which is more cost-effective and accessible than inkjet printing. Overall, our study presents a practical and straightforward process for fabricating high-quality flexible microheaters, which have the potential for use in various portable biomedical applications requiring reliable heat management solutions.

2. MATERIALS AND METHODS

2.1 Flexible Microheater Preparation

A polyimide (PI) substrate (DuPont, Delaware, USA), measuring 25 x 75 mm was immersed in a 4 M KOH solution (Sigma Aldrich, Saint Louis, USA) for 210 min to cleanse and activate its surface.

Subsequently, it was meticulously rinsed with deionized (DI) water to eliminate any remaining KOH or other impurities that could disrupt the following procedures. The PI substrate was then immersed in a 0.02 M $AgNO_3$ solution (Sigma Aldrich, Saint Louis, USA) for 30 min to deposit silver ions onto its surface, which were converted to metallic silver (Figure 1 step 1-4).

The microheater patterns were fabricated using an electronic craft cutter (Silhouette Portrait 3, Utah, USA) on a sticker sheet (Oracal, Oranienburg, Germany). The parameters of the electronic craft cutter were carefully adjusted to achieve high-precision patterns, which perfectly aligned with the pre-designed layout. The patterned sticker is carefully aligned and applied to the PI substrate, ensuring accurate positioning (Figure 1 step 5-6).

The PI substrate was placed on the sticker and then immersed in 0.5 mM $NaBH_4$ solution (Sigma Aldrich, Saint Louis, USA). This process involves the reduction of absorbed silver ions, resulting in the formation of a metallic silver layer that creates a conductive layer on the PI substrate (step 7). Subsequently, the doctor blade technique is employed to uniformly distribute our nanocomposite mixture (Ag-PVA 30%) over the patterned surface (step 8). PVA was purchased from Sigma-Aldrich (Darmstadt, Germany), and Ag in silver ink was purchased from MJ Chemical (Jakarta, Indonesia). This step results in the formation of a polyimide microheater after peeling away the sticker pattern.

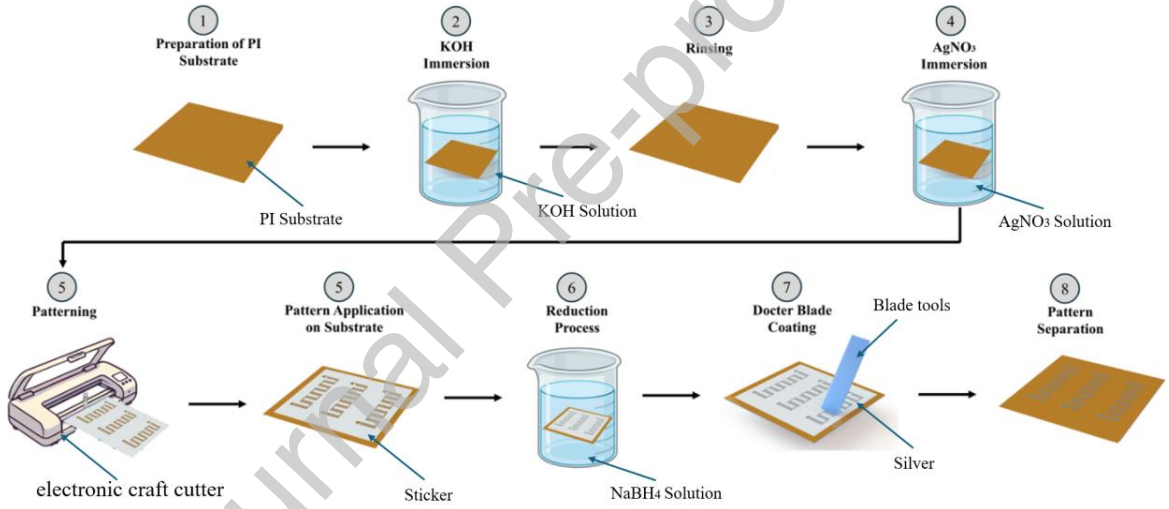

Figure 1. Preparation of a silver microheater on a flexible polyimide substrate using a combination of SMIE and doctor blade deposition

2.2 Flexible Microheater Characterization

The performance and characteristics of flexible silver heaters were evaluated using complementary characterization methodologies and categorized into multiple groups:

Geometry Characterization: The width of the electrodes was determined using a Dinolite AM4113 calibrated digital microscope (Anmo, New Taipei, Taiwan). An Accretech Surfcom 2900SD3 (Seimitsu, Tokyo, Japan) was used for the thickness and contour analysis.

Heating Performance Measurement: Joule heating was used to assess the heating capacity of the silver heater. The heater was linked to a DC power source (GW Instek, Taipei, Taiwan) to produce heat, and the temperature variations were measured in real time. The data were collected using a thermocouple

(TDK Electronics, Munich, Germany) linked to a National Instruments NI-USB 6001 module (Austin, TX, USA) within a four-channel data gathering system. Additionally, the temperatures recorded by the thermistors were corroborated using an infrared camera (FLIR Thermovision A320, Santa Barbara, CA, USA).

Thermal Properties and Stability: Differential Scanning Calorimetry (DSC) and Thermogravimetric Analysis (TGA) were employed to assess the thermal characteristics and stability, utilizing a Perkin Elmer DTA 4000 instrument (Waltham, MA, USA). Samples weighing approximately 15 mg were subjected to heating from ambient temperature to 800°C in a nitrogen environment at a flow rate of 30 mL/min.

Elemental Composition and Surface Morphology: The surface morphology and elemental composition of the heaters were analyzed using a Phenom ProX Desktop Scanning Electron Microscope (SEM) integrated with Energy Dispersive X-ray Spectroscopy (EDS) from Thermo Fisher Scientific Inc., Waltham, Massachusetts, USA. The porosity of the silver-PVA microheater was determined using image analysis techniques applied to Scanning Electron Microscopy (SEM) images. The SEM images were processed using ImageJ software. Grayscale images were first converted into binary format via Otsu's thresholding method to differentiate the silver matrix from the voids. The porosity percentage was then calculated as the ratio of the total pore area to the total analyzed electrode area.

Bending Characterization: The mechanical endurance and flexibility of the flexible heaters were evaluated by subjecting the substrates to numerous bending cycles using the mechanical dynamic testing apparatus Hung Ta HT-9501 (Taichung City, Taiwan). Resistance variations were quantified using the four-point probe technique during the bending cycles to evaluate the durability and dependability of the heaters.

Statistical analysis: This analysis was conducted to verify the reliability and reproducibility of the results. The essential procedures were gathering methodical data on temperature, resistance, and porosity, which were documented with precision. Descriptive statistics, such as mean, standard deviation, and confidence intervals, were computed for all measured parameters. Analysis of variance (ANOVA) was employed to evaluate the performance of heaters under various conditions, subsequently using Tukey's test to discern significant differences among distinct groups. The statistical study used Python 3, ensuring precise and thorough data interpretation. This study aims to comprehensively assess the efficacy of flexible silver microheaters and their appropriateness for biological applications through the use of various approaches and instruments.

3. RESULTS AND DISCUSSIONS

3.1 Geometry Characterization

Figure 2a illustrates the realization of a pattern that was successfully completed using a cross cutter machine on a sticker sheet. Figure 2b shows a polyimide substrate covered with a sticker sheet previously treated in series of SMIE to initiate polymer metallization. The silver/PVA microheater was successfully deposited by the doctor blade process of the polyimide substrate, as depicted in figure 2c. A flexible polyamide microheater was readily used and exhibited robust deposition, as shown in figure 2d.

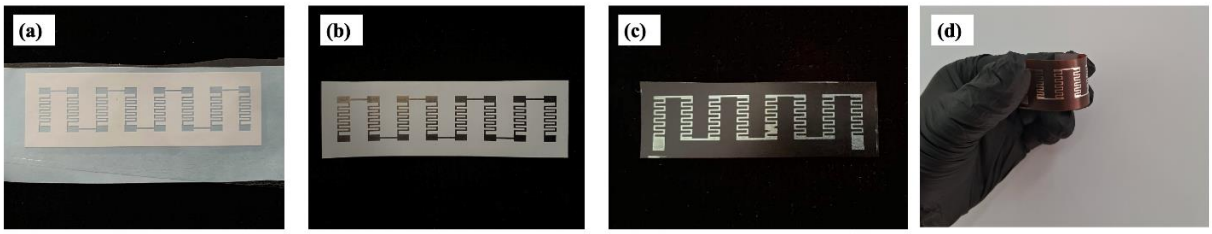

Figure 2. The realization of the heater from the pattern until testing: (a) the craft cutter-generated pattern, (b) the silver pattern with masking in place, (c) the silver pattern after mask removal, (d) the flexible heater demonstrating flexibility.

This study presents a comparison between the geometry of the masking (Figure 3a) and realized structure (Figure 3b), highlighting several dimensional differences. The fabricated masks exhibited horizontal and vertical dimensions of 2998 µm and 1200 µm, respectively, closely aligning with the designed dimensions of 3000 µm and 1200 µm. Nevertheless, minor discrepancies were noted in the smaller features, with a width of 293 µm and a vertical width of 557 µm in the constructed structure, as opposed to the theoretical values of 300 µm and 550 µm. The observed variations were closely aligned, remaining within a margin of 2.5% from the theoretical values.

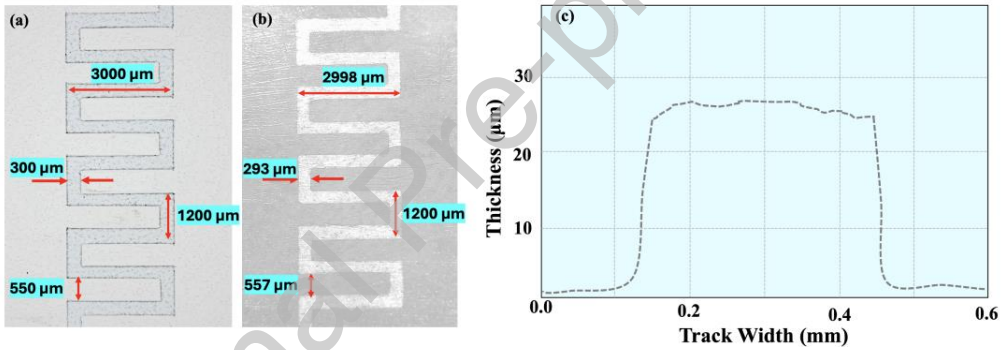

Figure 3. Close observation of the resulting (a) masking as the heater pattern, (b) realized heater after deposition, (c) profile measurement of the microheater

Our previous study (Whulanza et al., 2024) revealed variations of approximately 4%, achieved using a stencil mask without implementing the SMIE process. This notable enhancement is essential for biomedical applications. Variations in these dimensions can significantly influence the performance of devices such as microheaters used in the polymerase chain reaction on chips. Research indicates that even minor geometric discrepancies can influence the overall thermal and mechanical performance (Inaba et al., 2021; D. S. Lee et al. (2019). A common approach to addressing these challenges involves the application of traditional microfabrication techniques, including photolithography and lift-off processes. Nonetheless, these methods incur significant costs and necessitate equipment and facilities that may not be readily accessible, particularly in resource-limited environments. Our proposed solution effectively addresses these limitations.

The thickness measurement after the SMIE and coating process (figure 3c) revealed a channel microheater thickness of approximately 28 µm on the PI substrate, with a width of 300 µm and a sharp decrease in thickness at the edges of the track. The surface distribution suggests a texture variation, likely caused by the nonuniform ion-exchange reaction rate during the SMIE process and the different drying

rates of the silver - 30% PVA coating. These factors contribute to the material's uneven distribution, with thicker deposition occurring in the center and tapering off toward the edges. Additionally, the uneven surface texture of the microheater channel was attributed to the initially rough polyimide surface, which influenced the final material deposition.

3.2 Thermal Properties and Stability

The thermal evaluation of the flexible silver heater was conducted by thermogravimetric analysis (TGA) and Differential Scanning Calorimetry (DSC). Figure 4a shows the TGA curves for the substrate polyimide (PI) along with the substrate integrated with the silver heater. The TGA curves illustrate the relationship between the weight loss of the materials and temperature, providing insights into their thermal stability and decomposition points. The PI substrate exhibits two notable weight losses: at temperature around 100^{o}C, which is primarily due to water or solvent loss, whereas the weight loss beginning at approximately 500°C is due to the initiation of thermal decomposition. The substrate containing the silver heater exhibited solvent loss at temperature more than 150^{o}C and a significantly elevated decomposition temperature around 600^{o}C, indicating improved thermal stability attributed to the silver metallization.

Figure 4b shows the DSC curves for both the PI substrate and the substrate integrated with the silver heater. Both the PI substrates and those containing Ag heaters exhibited endothermic peaks at approximately 175°C, which suggests solvent evaporation and the release of chemically bound water.The exothermic peak at approximately 580^{o}C of the PI substrates indicates the decomposition temperature (Akinyi & Iroh, 2023). Meanwhile, the PI substrate with the silver heater exhibited a higher exothermic peak at 620^{o}C.

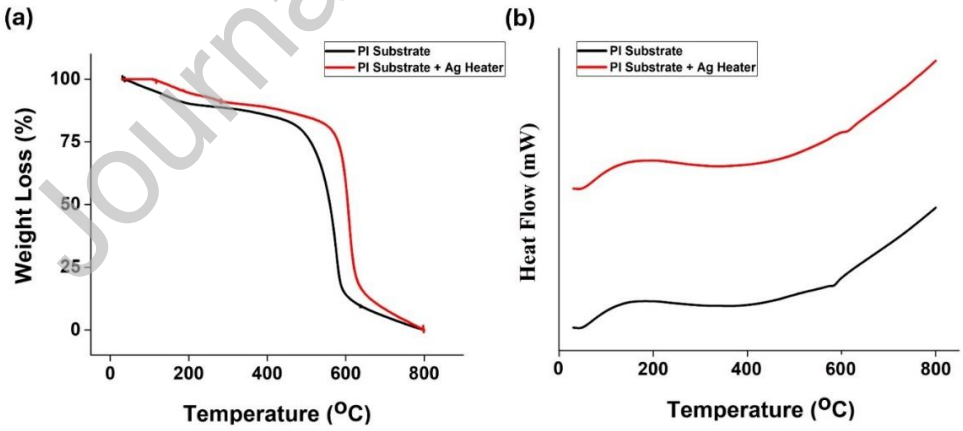

Figure 4: (a) Thermogravimetric analysis (TGA) and (b) Differential scanning calorimetry (DSC) results for a polyimide substrate with and without silver deposition.

Based on the thermal characteristics above, the addition of silver clearly improves the thermal stability of the polyimide substrate. This is presumed to be due to the combination effect of the deposited silver particles after ion-exchange metallization and ion-dipole interaction between the silver ions (Ag^{+})

and the PVA polymer chain.(S. Y. Lee et al. (2021) revealed that the polar hydroxy groups of hydroxy polyimide established ion-dipole interactions with Ag ions, resulting in the formation of Ag particles with a homogeneous size distribution. This interaction may also be exhibited in our Ag-PVA composite because PVA contains hydroxyl groups. As a result, the distribution of Ag influences the heat emission properties of the composite film, leading to improved heat dissipation and greater thermal stability.

Elevated melting points and decomposition temperatures are crucial for applications involving prolonged heating, which generally occur below 100°C in the medical field. In summary, the higher melting point and thermal stability of the substrate with silver compared to the PI substrate alone demonstrate the benefits of silver metallization, enhancing reliability and performance for applications like biomedical devices and wearable technology (Mitra et al., 2022).

3.2 Heating performance measurements

Testing of the flexible heater was conducted as shown in Figure 5a, which illustrates the thermal scanner of the upper surface of the polyimide substrate, while figure 5b depicts the perspective from the lower section.

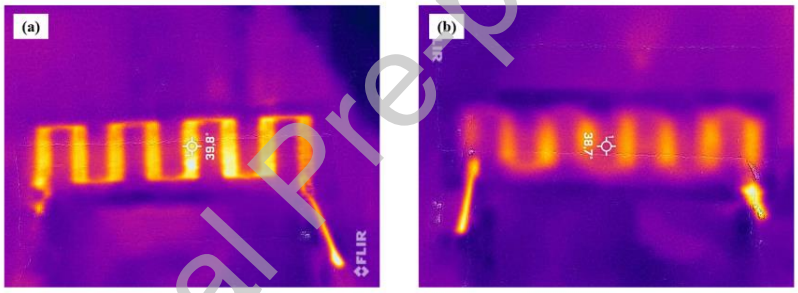

Figure 5. (a) thermal imaging of the heater at the top section and (b) thermal imaging of the heater at the bottom section.

The performance of the flexible silver heater was also assessed at various constant DC voltage levels. Figure 6a illustrates the temperature curves over time at different voltage levels (0.50 V, 0.75 V, 1.00 V, 1.25 V, and 1.50 V). The findings demonstrate that with an increase in applied voltage, there is a notable increase in both the rate of temperature increase and the maximum temperature reached. At 1.50 V, the heater reached a temperature of around 160°C, indicating a swift response and significant heating efficiency. ANOVA for maximum temperature revealed a statistically significant difference in heat flux density among various voltage levels ($F(4, 20) = 10513.09$, $p = 0.0001$, $N = 25$, $R^2 = 0.92$, Adjusted $R^2 = 0.91$). These results confirm that the model explains a substantial proportion of the variance in heat flux density at different voltage levels. The results of the Tukey test reinforce this observation, indicating that higher voltages result in notable variations in the maximum temperature attained.

Figure 6b illustrates the peak temperature at each voltage level, demonstrating a distinct relationship between the applied voltage and the corresponding temperature outcome. The data indicate a consistent increase in temperature corresponding to elevated voltages, implying effective heating capabilities. Figure 6c presents a detailed examination of the temperature stability over a 60-min period,

demonstrating consistent temperature maintenance across different voltage levels, with 1.50 V achieving the peak temperature just under 160°C.

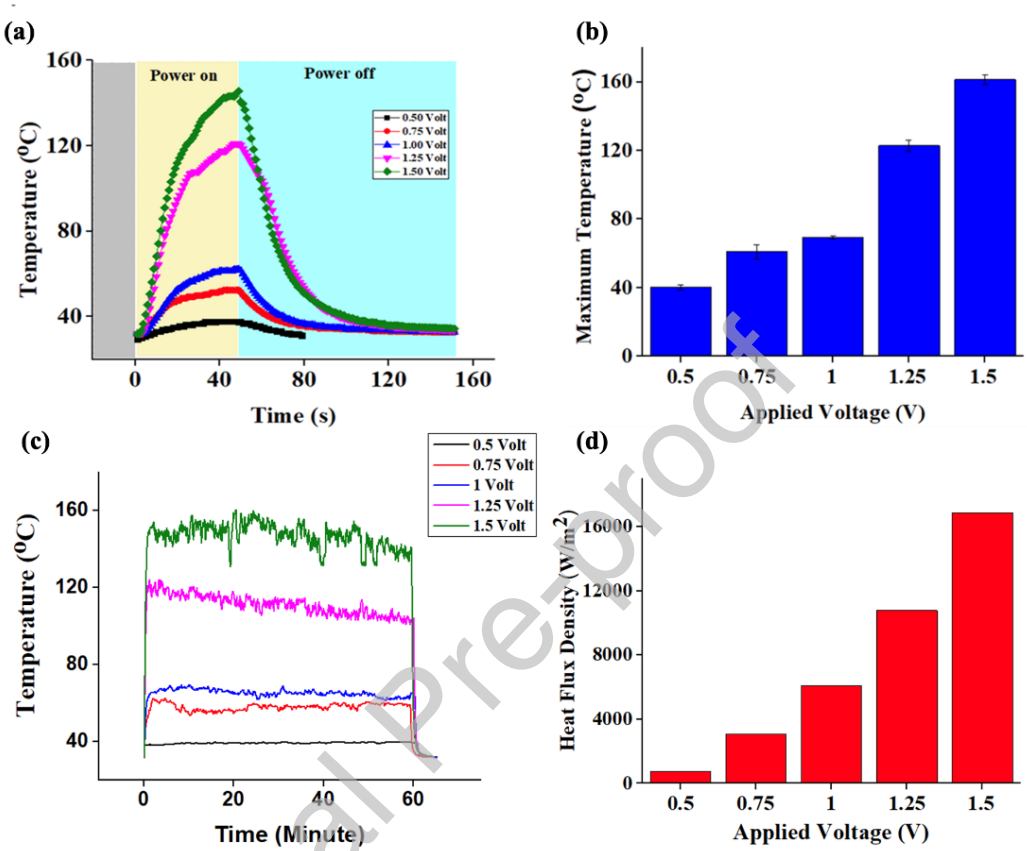

Figure 6. (a) Time-dependent temperature curves of the flexible silver heater at various applied voltages; (b) graph showing the maximum temperature achieved by the flexible silver heater at different applied voltages; (c) steady-state temperature stability of the flexible silver heater at different applied voltages over time; (d) heat flux density vs. voltage.

The heating rate was calculated from the slope of the temperature–time curve during the linear phase (25–90% of the maximum temperature, T_{max}). At 1.50 V, the microheater achieved a heating rate of 11.9 ± 1.1°C/s, reaching 160°C within 13.5 seconds. Lower voltages yielded proportionally slower rates (e.g., 2.1°C/s at 0.50 V), demonstrating the device's tunability for diverse applications. After power disconnection at 1.50 V, the temperature dropped from 160°C to 50°C within 18 s, yielding an average cooling rate of 6.1°C/s. This efficiency is attributed to the low thermal mass (28 µm thickness) and thermal conductivity (0.12 W/m·K).

The analysis of the steady-state temperature reveals that the heater sustains a uniform temperature over extended durations, which is essential for applications requiring stable thermal conditions. Notable variations were detected at elevated voltages, especially at 1.50 V, suggesting the heater's difficulty in consistently sustaining high temperatures. This indicates that at elevated voltages, the heater performance appears to exhibit instability, necessitating additional assessment to improve its reliability in real-world applications. The increase in heat flux density corresponding to elevated voltages, as illustrated in Figure

6d, underscores the heater's effectiveness in transforming electrical energy into thermal energy. The significance of this efficiency lies in its potential to enhance energy savings and reduce operational costs in practical applications. The consistent heat distribution noted across the heater surface reinforces its suitability for applications requiring reliable thermal management, including wearable devices and defogging systems (Guo et al., 2020; Z. Hu et al. (2021)

3.3 Elemental Composition and Surface Morphology

The analyses of the surface morphology and elemental composition of the flexible silver heater, conducted through Scanning Electron Microscopy (SEM) and energy-dispersive X-ray Spectroscopy (EDS), provide important insights into the impact of the heating process on our microheaters. Figure 7c displays SEM images of the microheaters' surfaces following the application of different voltages (0.5 V, 0.75 V, 1.0 V, 1.25 V, and 1.5 V), highlighting both the original images and those subjected to image processing. The images indicate a more consistent distribution of silver particles at elevated voltages, accompanied by a reduction in porosity as the voltage rises. The observations correspond with the ANOVA test results, demonstrating a statistically significant effect of voltage on porosity ($F(4, 20) = 34.66$, $p = 0.0008$, $N = 25$, $R^2 = 0.88$, Adjusted $R^2 = 0.86$), thereby validating the differences in porosity at various voltage levels.

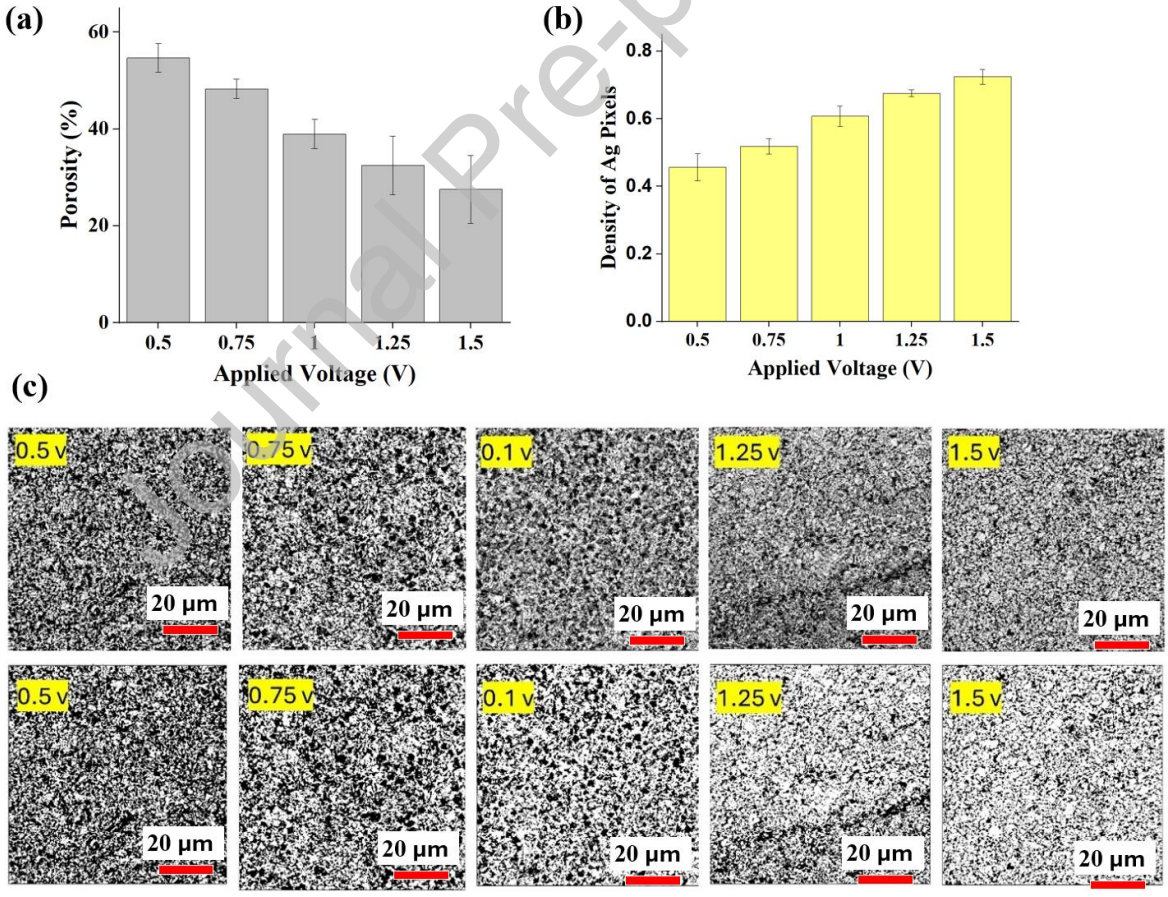

Figure 7: (a) Graph indicating the porosity of the flexible silver heater at different applied voltages; (b) density of silver pixels vs. applied voltage; (c) SEM images showing the surface morphology of the flexible silver heater at different applied voltages (original SEM images on top, processed images below)

Figure 7a illustrates the relationship between porosity and voltage, indicating a decline in porosity with increasing voltage. The observed trend indicates that increased voltages lead to a denser and more compact distribution of silver particles. Figure 7b. The density of Ag pixels represents the proportion of silver (Ag) pixels relative to the total number of pixels in the image. This metric indicates the extent to which silver pixels occupy the image area. As the applied voltage increases, the density of Ag pixels also increases, suggesting a direct relationship between voltage and the deposition or distribution of silver particles. Higher voltages contribute to a more concentrated presence of Ag pixels, which can be critical for understanding the behavior of materials under different electrical conditions.

The EDS analysis table in Table 1 compares the elemental compositions of the heaters at 0 V and 1.5 V. The findings show a rise in the silver content from 53.06% to 74.11%, accompanied by a reduction in organic elements such as carbon, oxygen, and hydrogen. This implies organic degradation alongside enhanced silver deposition at elevated voltages. The reduction in porosity and consistent distribution of silver particles at elevated voltages improve the electrical and thermal characteristics of the heater. An arrangement of denser silver particles enhances both the conductivity and the heat transfer efficiency. The reduction in porosity with increasing voltage (Figure 8a) reinforces this observation, indicating a more compact and efficient conductive network.

Table 1 EDS analysis of the elemental composition of the flexible silver heater before and after heating at different voltages.

Element	0 Volt	1.5 volt
Silver	53.06%	74.11%
Carbon	14.41%	10.45%
Oxygen	22,53%	11.03%
Hydrogen	10%	4.41%

The EDS analysis presented in Table 1 shows an increase in the silver content from 53.06% to 74.11% with increasing voltage, whereas organic elements such as carbon and oxygen decrease. This trend indicates that higher voltage facilitates denser silver deposition and the degradation of organic materials, enhancing the electrical and thermal properties of the microheater. This phenomenon can be explained by several mechanisms. First, a higher voltage accelerates the evaporation of organic residues due to increased thermal energy, resulting in a more crystalline silver layer. Second, the XRD analysis (figure 8) reveals increased silver crystallinity at higher voltages, indicating a more organized and conductive silver network. Third, SEM images (figure 7) show a reduction in porosity, reflecting a denser and more uniform silver distribution. The improved silver deposition enhanced the performance of the heater by increasing its thermal and electrical conductivity, which is consistent with the results of previous research on silver nanowires and conductive materials (Cheng et al., 2016; Liu et al., 2015).

The flexible silver heater through X-ray diffraction (XRD) was conducted to identify the crystalline phases and assess the degree of crystallinity. The XRD patterns of the microheaters at various voltages (0.5 V, 0.75 V, 1.0 V, 1.25 V, and 1.5 V) are presented in Figure 8. The observed peaks align with the crystalline structures of silver, demonstrating an increase in peak intensity corresponding to

higher applied voltages. This suggests that elevated voltages increase the crystallinity. The XRD patterns show clear peaks at particular angles, suggesting the presence of crystalline silver. The increase in voltage correlated with a rise in the intensity of these peaks, indicating a potential enhancement in crystallinity and improvement in material quality. The decrease in the organic peak intensity provides additional evidence for the degradation of organic components observed through EDS analysis (as mentioned above).

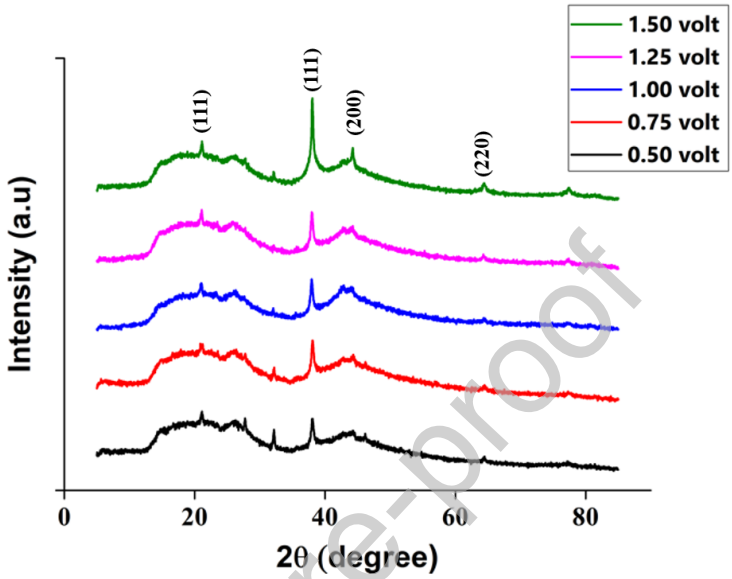

Figure 8. XRD patterns of flexible silver heaters at various applied voltages

The crystalline phases observed in the XRD patterns play a crucial role in improving the thermal and electrical properties of heaters. The presence of crystalline silver, as evidenced by the XRD peaks, demonstrates an enhanced conductivity relative to that of its amorphous form. The observation of higher peak intensities at elevated voltages indicates an enhanced crystallinity, which is associated with improved performance. This result is consistent with EDS data, which indicated that increased silver content and decreased organic elements at elevated voltages lead to enhanced efficiency in practical applications (Sun et al., 2018; Tian et al., 2023).

The results agree with earlier research (Whulanza et al., 2024), indicating that crystalline silver exhibits improved conductivity compared to its amorphous counterparts. The heightened crystallinity observed at elevated voltages corroborates this, indicating a more organized atomic structure that enhances performance and longevity. The pronounced XRD peaks suggest a high-quality material, which is crucial for ensuring long-term stability, as evidenced by research on conductive materials such as silver (Mulenga et al., 2020; Priotto et al., 2023).

3.4 Mechanical Durability

The structural integrity of silver deposited on the substrate is a critical aspect of this field. The proposed method employs a robust silver component within the substrate. This paper presents an observation of the change in resistance of the flexible silver heater when subjected to prolonged external forces. The force is represented by a series of bending forces applied over 5000 cycles, as illustrated in Figure 9. The data indicate a minor but consistent reduction in resistance, which decreases from 223.9 Ω to 220.9 Ω across 5000 bending cycles, with no notable thermal degradation evident in the thermal

infrared images. An ANOVA test ($F(4, 20) = 34.9$, $p = 0.0001$, $N = 25$, $R^2 = 0.89$, Adjusted $R^2 = 0.87$) followed by Tukey's HSD test revealed significant differences among specific voltage groups, underscoring the material's durability and limited fatigue during repeated bending.

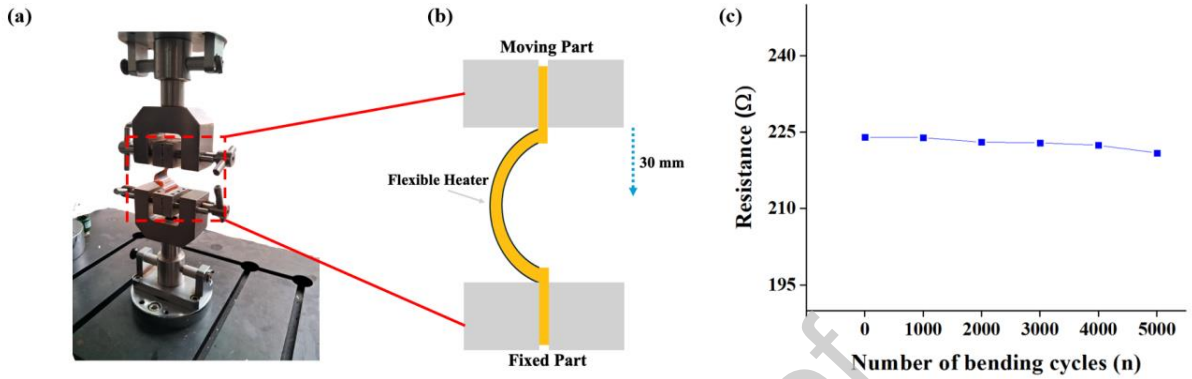

Figure 9. (a) Experimental setup for bending test of flexible microheater. (b) Illustration of bending dynamics in flexible microheater. (c) graph showing the change in resistance of flexible microheater with increasing number of bending cycles.

The observed gradual decrease in resistance from 223.9 Ω to 220.9 Ω over 5000 bending cycles, which is less than 1% variation, indicates the heater's robust mechanical properties. This minimal reduction is consistent with the known behavior of flexible heaters, where microcracks and molecular reorientation influence resistance changes (Huang et al., 2015). The thermal infrared images corroborate these findings, showing stable thermal performance without noticeable hotspots or degradation. Studies on materials like Bi2Se3-MWCNT and Ag nanowire networks also support these observations, emphasizing the role of material quality and structural integrity in maintaining performance (Bugovecka et al., 2023; Hwang et al., 2021).

The mechanical stability of the flexible silver heater is comparable to those of other flexible conductive materials, including silver nanowires, carbon nanotubes, and graphene, which demonstrate robust flexibility and maintain performance under mechanical stress (Z. Hu et al., 2021; Jin et al., 2021; Kim et al., 2021). In contrast, certain materials exhibit significant resistance changes under stress due to microcracks, which negatively affect their performance (Park et al., 2019). However, the flexible nanocomposite silver heater exhibits enhanced durability by maintaining or reducing resistance during repeated bending, making it suitable for applications requiring long-term reliability and consistent performance, such as wearable electronics.(Y. Hu et al., 2022; Sharma et al., 2020; N. Zhang, Huang, Wan, Lee, et al., 2019).

Additionally, its performance during repeated bending cycles aligns with the results of research on comparable materials, underscoring its mechanical strength (Jin et al., 2021; J. Yang et al., 2021). The heater exhibits a resistance change ratio of 0.11% after 1200 cycles, indicating exceptional stability, which is particularly significant for applications in flexible electronics and biomedicine. The findings highlight the necessity of creating flexible heaters capable of withstanding mechanical stress while maintaining their functionality, which corresponds to the need for robust thermal management solutions across multiple sectors.

3.5 Temperature Coefficient of Resistance (TCR)

The electrical resistance of the microheater was evaluated at various temperatures and under mechanical bending conditions. The resistance at room temperature (25°C ± 1°C) was measured as 223.9 Ω. The resistance-temperature relationship followed the TCR model with an experimentally derived coefficient of $\alpha = 0.0031\ °C^{-1}$. The calculated and measured resistance values at different temperatures exhibited strong agreement, as shown in Table 2.

Table 2. Measured vs. Calculated Resistance Values

Temperature (°C)	**Calculated R (Ω)**	**Measured R*R* (Ω)**	**Deviation (%)**
25	223.9	223.9 ± 0.5	0.0
40	231.2	230.5 ± 0.7	0.3
60	240.1	238.9 ± 1.1	0.5

The experimental results validate the theoretical predictions of the microheater's electrical behavior as a function of temperature. The close agreement between the calculated and measured resistance values supports the accuracy of the TCR model for silver-based conductive films. The deviation remained within 1% across the tested temperature range (25–60°C), demonstrating the precision of the measurement process and the reliability of the microheater's design. The minimal resistance degradation observed after mechanical bending suggests that the microheater exhibits high mechanical durability. This result can be attributed to the strong adhesion properties of the SMIE and the inherent flexibility of the Ag-PVA nanocomposite material. These characteristics make the microheater a strong candidate for flexible and wearable electronics, where mechanical stress is inevitable.

Moreover, the additional analysis of resistance variations during bending cycles provides insights into the microheater's longevity and operational stability. Given that the resistance decrease was minor and remained within acceptable limits, it can be inferred that the structural integrity of the conductive pathway is preserved even under repeated deformation. Overall, the findings presented in this study confirm the robustness, reliability, and reproducibility of the microheater's electrical properties. The combination of excellent temperature response and mechanical resilience makes it suitable for flexible next-generation flexible thermal management applications. Future work may involve testing under dynamic environmental conditions and exploring further material optimizations to enhance the operational lifespan.

3.6 Bioreactor Temperature Stability Test

To validate the microheater's applicability in bioreactor systems requiring precise thermal control, we conducted a temperature stability test using a water-filled chamber (20 mL volume) under ambient conditions. The microheater, powered by a 0.5 V battery and regulated by a voltage controller, was integrated beneath the chamber to simulate a bioreactor environment (Figure 10a). The system was programmed to maintain a target temperature of 40.0°C, which is critical for enzymatic reactions and mesophilic microbial processes. Temperature data were recorded for over 1 h using three calibrated thermocouples positioned at the top, center, and bottom of the chamber to evaluate spatial uniformity (Figure 10b).

The microheater demonstrated rapid heating, achieving the target temperature of 40.0°C within 4.2 minutes (heating rate: 9.5°C/min). During the 1-h operation, the temperature remained stable at 40.0 ± 0.1°C (Figure 10c) with minimal spatial variation (±0.2°C).

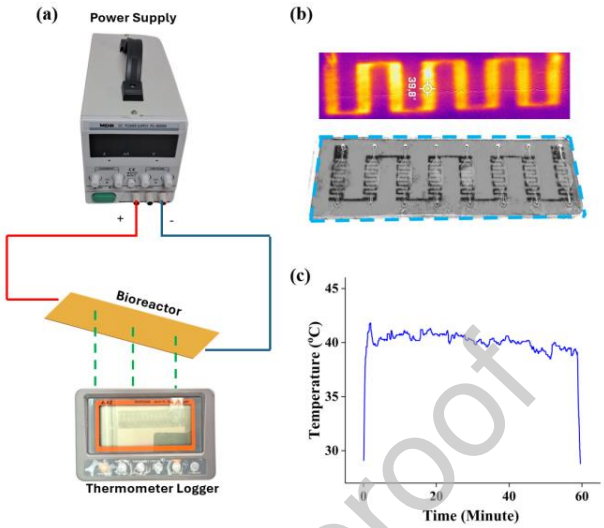

Figure 10. (a) Experimental setup of controlled environment in an bioreactor chip. (b) The application of silver heater on the chip. (c) Graph showing the temperature of heated liquid medium in the bioreactor chip.

These results confirm the microheater's suitability for applications demanding rapid and stable thermal regulation, such as enzymatic hydrolysis, biogas production, or batch fermentation. The portability of the battery-powered setup further underscores its potential for decentralized bioreactor systems in resource-limited settings. Future work will explore the integration of microbial cultures with real-time feedback control to assess biological efficacy under dynamic conditions.

3.7 Discussions

The combination of the SMIE technique and doctor blade coating successfully enabled the realization of a flexible heater with superior precision, stability, and durability compared to previous silver-based flexible heater designs. With only a 2.5% deviation from the theoretical values, the dimensional accuracy was significantly improved over previous studies, which can be largely attributed to the SMIE process. Although the thickness distribution (peaks at 28 µm) indicated some non-uniform material deposition leading to minor inconsistencies in the heat distribution, the heater maintained excellent overall performance.

The integration of silver enhanced material uniformity and operational stability. Thermal analysis using TGA and DSC further confirmed the improved performance, with silver increasing both the decomposition temperature and melting point of the polyimide substrate and enhancing thermal stability up to 170°C. The heating efficiency increased with the voltage, although the minor instability at 1.50 V suggested room for optimization at higher voltage operations. The rapid thermal response of the heater,

which is essential for energy efficiency, demonstrated silver's superiority in heat transfer. The mechanical durability was also notable, with the resistance variation remaining below 1% after 5000 bending cycles.

This research successfully addressed adhesion issues encountered in previous studies. The SMIE technique effectively metalized the substrate, forming a chemical bond between the polyimide (PI) substrate and the silver. This is primarily due to the SMIE method, in which the initially neutral PI substrate is modified with potassium hydroxide (KOH). This reaction replaces some functional groups on the polymer with potassium ions (K^+), creating sites that are ready for exchange with metal ions. This step is crucial for the PI substrate to absorb silver ions (figure 11).

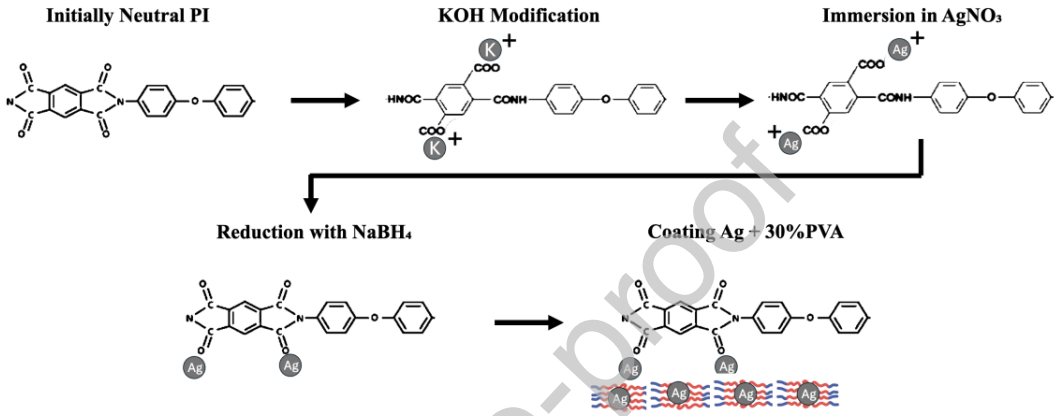

Figure 11. Changing of the chemical group and formation of silver on the PI (polyimide) surface.

After KOH modification, the PI substrate is immersed in a silver nitrate ($AgNO_3$) solution. During this process, potassium ions (K^+) are replaced by silver ions (Ag^+). As a result, the carboxylate groups ($-COO^-$) attached to the PI substrate now bind with Ag^+, replacing the K^+ ions. The bound Ag^+ ions are then reduced to elemental silver particles (Ag^0) using sodium borohydride ($NaBH_4$) as the reducing agent. This reaction converts the silver ions into their stable metallic form (Ag^0), which then integrates into the polymer structure. This combination of techniques ensures strong adhesion between the silver and the PI substrate, resolving the adhesion issues that have been a challenge in previous research.

The proposed surface modification ion exchange (SMIE) and doctor blade deposition method offers a low-cost alternative to traditional cleanroom-based photolithography, which typically requires high-cost lithography tools (> $50,000), photoresists, masks, and chemical etchants. By eliminating the need for expensive equipment and complex multi-step processing, the proposed method reduces fabrication costs by over 90%, lowers material consumption by ~60-80%, and minimizes waste generation by ~70%, making it a more scalable and environmentally friendly approach. Additionally, the simplified fabrication process enables continuous and large-area production, which is not feasible with traditional batch-based photolithography. These advantages demonstrate that our method is a cost-effective, efficient, and sustainable alternative for flexible microheater fabrication, justifying its potential for biomedical and electronic applications (Charmet et al., 2020).

4. CONCLUSION

This study developed and evaluated a novel flexible nanocomposite silver microheater using a solution-based polyimide metallization technique combined with an electronic craft cutter, achieving

enhanced thermal performance, response time, and mechanical stability for biomedical applications. The microheaters exhibited excellent thermal properties, with the decomposition temperature of the nanocomposite silver-metalized polyimide substrate reaching approximately 620°C. The integration of silver significantly enhanced thermal stability, as evidenced by higher decomposition temperatures in TGA analysis. DSC curves confirmed endothermic events corresponding to phase transitions, highlighting the material's robustness for high-temperature applications. The heating performance tests showed rapid temperature increases, reaching approximately 160°C at 1.50 V and stable temperatures over extended periods, underscoring their suitability for applications requiring consistent thermal management.

CRediT authorship contribution statement

Deni Haryadi: Conceptualization, Formal analysis, Methodology, Software, Visualization, Validation, Writing– original draft, Writing– review & editing. **Yudan Whulanza:** Conceptualization, Methodology, Investigation, Supervision, Funding acquisition, Writing– review & editing. **Jerome Charmet:** Supervision, Writing– review & editing, Funding acquisition. **Bambang Suryawan:** Writing– review & editing, Formal analysis. **Jos Istiyanto**: Writing– review & editing, Funding acquisition. **Azizah Intan Pangesty:** Methodology, Writing– review & editing, **Sugeng Supriadi**: Methodology, Writing– review & editing.

Declaration of Competing Interest

The authors declare that they have no known competing financial interests or personal relationships that could have appeared to influence the work reported in this paper.

Declaration of generative AI and AI-assisted technologies in the writing process

During the preparation of this work, the authors used QuillBot.com to refine the spelling and wording of the paragraph. After using this tool/service, the authors reviewed and edited the content as needed and take full responsibility for the content of the publication.

Acknowledgements

The research is funded by grant of University of Indonesia PUTI Grant 2025. The scholarship of the main author was funded by University Gunadarma Post Graduate Program 2024.

REREFERENCES

Akinyi, C., & Iroh, J. O. (2023). Thermal Decomposition and Stability of Hybrid Graphene–Clay/Polyimide Nanocomposites. *Polymers*, *15*(2). https://doi.org/10.3390/polym15020299

Aleksandrova, M., Ustova, B., Tsanev, T., Raptis, I., Tserepi, A., Gogolides, E., & Kolev, G. (2024). Microheater Topology for Advanced Gas Sensor Applications with Carbyne-Enriched Nanomaterials. *Applied Sciences (Switzerland)*, *14*(5). https://doi.org/10.3390/app14051728

Al-Mohsin, H., Ali, S., & Bermak, A. (2022). Design and Fabrication Process Optimization of Silver-Based Inkjet-Printed Microheater. *Processes*, *10*(9). https://doi.org/10.3390/pr10091677

Andreozzi, A., Brunese, L., Iasiello, M., Tucci, C., & Vanoli, G. P. (2022). A New Thermal Damage-Controlled Protocol for Thermal Ablation Modeled with Modified Porous Media-Based Bioheat Equation with Variable Porosity. *Processes*, *10*(2). https://doi.org/10.3390/pr10020236

Barman, U., Wiederkehr, R. S., Fiorini, P., Lagae, L., & Jones, B. (2018). A comprehensive methodology for design and development of an integrated microheater for on-chip DNA amplification. *Journal of Micromechanics and Microengineering*, *28*(8). https://doi.org/10.1088/1361-6439/aabd2c

Bugovecka, L., Buks, K., Andzane, J., Miezubrale, A. D., Bitenieks, J., Zicāns, J., & Erts, D. (2023). Positive and Negative Changes in the Electrical Conductance Related to Hybrid Filler Distribution Gradient in Composite Flexible Thermoelectric Films Subjected to Bending. *Nanomaterials*, *13*(7), 1212. https://doi.org/10.3390/nano13071212

Byers, K. M., Lin, L. K., Moehling, T. J., Stanciu, L., & Linnes, J. C. (2020). Versatile printed microheaters to enable low-power thermal control in paper diagnostics. *Analyst*, *145*(1). https://doi.org/10.1039/c9an01546a

Charmet, J., Rodrigues, R., Yildirim, E., Challa, P. K., Roberts, B., Dallmann, R., & Whulanza, Y. (2020). Low-Cost microfabrication tool box. *Micromachines*, *11*(2). https://doi.org/10.3390/mi11020135

Gu, X., Li, D. D., Yeoh, G. H., Taylor, R. A., & Timchenko, V. (2021). Heat generation in irradiated gold nanoparticle solutions for hyperthermia applications. *Processes*, *9*(2). https://doi.org/10.3390/pr9020368

Guo, Z., Sun, C., Zhao, J., Cai, Z., & Ge, F. (2020). Low-Voltage Electrical Heater Based on One-Step Fabrication of Conductive Cu Nanowire Networks for Application in Wearable Devices. *Advanced Materials Interfaces*, *8*(3). https://doi.org/10.1002/admi.202001695

Hou, X., & Zhang, J. (2018). Fully Inkjet-Printed Acetone Gas Sensors on Flexible Substrates with Integrated Heater for Sensing Material in-situ Deposition and Elevated Temperature Detection. *Chinese Journal of Sensors and Actuators*, *31*(4). https://doi.org/10.3969/j.issn.1004-1699.2018.04.002

Hu, Y., Zhang, Z., Zhang, D., Xiu, F., Zhang, M., Dong, X., Cheng, S., Zhang, Z., Chen, C., Xie, X., Liu, J., & Huang, W. (2022). Adaptive and Remote Thermoregulation ofEnabled With a Highly Stable Transparent Flexible Heating Film. *Acs Applied Energy Materials*, *5*(7), 8892–8899. https://doi.org/10.1021/acsaem.2c01379

Hu, Z., Zhou, J., & Fu, Q. (2021a). Design and Construction of Deformable Heaters: Materials, Structure, and Applications. *Advanced Electronic Materials*, *7*(11). https://doi.org/10.1002/aelm.202100459

Hu, Z., Zhou, J., & Fu, Q. (2021b). Design and Construction of Deformable Heaters: Materials, structuresStructure, and Applications. *Advanced Electronic Materials*, *7*(11). https://doi.org/10.1002/aelm.202100459

Huang, Q., Shen, W., Fang, X., Chen, G., Guo, J., Xü, W., Tan, R., & Song, W. (2015). Highly Flexible and Transparent Film Heaters Based on Polyimide Films Embedded With Silver Nanowires. *RSC Advances*, *5*(57), 45836–45842. https://doi.org/10.1039/c5ra06529a

Hwang, J. S., Park, J.-E., Kim, G. W., Nam, H., Yu, S., Jeon, J. S., Kim, S., Lee, H. S., & Yang, M. (2021). Recycling Silver Nanoparticle Debris From Laser Ablation of Silver Nanowire in Liquid Media Toward Minimum Material Waste. *Scientific Reports*. *11*(1). https://doi.org/10.1038/s41598-021-81692-9

Inaba, M., Higashimoto, Y., Toyama, Y., Horiguchi, T., Hibino, M., Iwata, M., Imaizumi, K., & Doi, Y. (2021). Diagnostic accuracy of LAMP versus PCR over the course of SARS-CoV-2 infection. *International Journal of Infectious Diseases*, *107*. https://doi.org/10.1016/j.ijid.2021.04.018

Irwansyah, R., Juana, F., Whulanza, Y., & Charmet, J. (2021). Heating Characterization of Low Energy Consumption Lab-on-a-Chip. *Evergreen*, *8*(4). https://doi.org/10.5109/4742135

Jin, I. S., Lee, H. D., Hong, S. I., Lee, W., & Jung, J. W. (2021a). Facile Post Treatment of Ag Nanowire/Polymer Composites for Flexible Transparent Electrodes and Thin Film Heaters. *Polymers*, *13*(4), 586. https://doi.org/10.3390/polym13040586

Jin, I. S., Lee, H. D., Hong, S. I., Lee, W., & Jung, J. W. (2021b). Facile Post Treatment of Ag Nanowire/Polymer Composites for Flexible Transparent Electrodes and Thin Film Heaters. *Polymers*, *13*(4), 586. https://doi.org/10.3390/polym13040586

Josephin, A., Whulanza, Y., Rahman, S. F., Lischer, K., Surya, M. I., Martiansyah, I., Rahman, W., & Hashim, U. (2024). Easy extraction of Ganoderma boninense liquid sample using portable on-chip device. *Indonesian Journal of Biotechnology*, *29*(1), 33–39.

Kim, S. Y., Shin, W. H., Kim, H. S., Jung, D. W., Kim, M. J., Kim, K., Roh, J. W., Hwang, S., Lee, J., Yang, D., Sohn, H., Kim, S. H., Jung, C. W., Cho, E., Yun, D. J., Kim, J. H., Cho, Y. J., Kim, S. I., Lee, K. H., … Ko, D. S. (2021). Silver Nanowire Network Hybridized With Silver Nanoparticle-Anchored Ruthenium Oxide Nanosheets for Foldable Transparent Conductive Electrodes. *Acs Applied Materials & Interfaces*, *13*(9), 11396–11402. https://doi.org/10.1021/acsami.0c19471

Kitagawa, Y., Orihara, Y., Kawamura, R., Imai, K., Sakai, J., Tarumoto, N., Matsuoka, M., Takeuchi, S., Maesaki, S., & Maeda, T. (2020). Evaluation of rapid diagnosis of novel coronavirus disease (COVID-19) using loop-mediated isothermal amplification. *Journal of Clinical Virology*, *129*. https://doi.org/10.1016/j.jcv.2020.104446

Lee, B., Cho, I., Kang, M., Yang, D., & Park, I. (2023). Thermally/mechanically robust anodic aluminum oxide (AAO) microheater platform for low power chemoresistive gas sensor. *Journal of Micromechanics and Microengineering*, *33*(8). https://doi.org/10.1088/1361-6439/ace05e

Lee, D. S., Choi, O. R., & Seo, Y. (2019). A microheater on polyimide substrate for hand-held realtime microfluidic polymerase chain reaction amplification. *Micro and Nano Systems Letters*, *7*(1). https://doi.org/10.1186/s40486-019-0098-1

Lee, S. Y., Huh, T.-H., Jeong, H. R., Kwark, Y.-J. (2021). In situ fabrication of silver/polyimide composite films with enhanced heat dissipation. *RSC Advances*, *11*(43), 26546–26553.

Li, D., Ruan, Y., Chen, C., He, W., Chi, C., & Lin, Q. (2022). Design and thermal analysis of flexible microheaters. *Micromachines*, *13*(7), 1037.

Lischer, K., Putra, A. B. R. D., Sahlan, M., Khayrani, A. C., Ginting, M. J., Wijanarko, A., Whulanza, Y., & Pratami, D. K. (2021). Heat Transfer Simulation of MaterialsVarious Material for Polymerase Chain Reaction Thermal Cycler. *Journal of Mechanical Engineering*, *18*(2).

Mitra, D., Grummt, A., Thalheim, R., & Zichner, R. (2022). Reliability and Potential of Inkjet-Printed Flexible Heaters With Adaptive Temperature Zones for High-Temperature and Long-Time Applications. *Energy Technology*, *11*(2). https://doi.org/10.1002/ente.202200874

Mulenga, G. M., Henning, L., Chilongo, K., Mubamba, C., Namangala, B., & Gummow, B. (2020). Insights into the control and management of human and bovine african trypanosomiasis in zambia between 2009 and 2019-a review. In *Tropical Medicine and Infectious Disease* (Vol. 5, Issue 3). https://doi.org/10.3390/tropicalmed5030115

Nadhif, M. H., Whulanza, Y., Istiyanto, J., & Bachtiar, B. M. (2017). Delivery of Amphotericin B to Candida albicans by using biomachined lab-on-A-chip. *Journal of Biomimetics, Biomaterials and Biomedical Engineering*, *30*. https://doi.org/10.4028/www.scientific.net/JBBBE.30.24

Park, J., Han, D.-J., Choi, S.-H., Kim, Y.-K., & Kwak, J. (2019). Flexible Transparent Film Heaters Using a Ternary Composite of Silver Nanowire, Conducting Polymer, and Conductive Oxide. *RSC Advances*, *9*(10), 5731–5737. https://doi.org/10.1039/c9ra00341j

Priotto, G., Franco, J. R., Lejon, V., Büscher, P., Matovu, E., Ndung'u, J., Biéler, S., Mumba, D., Reet, N. Van, Verlé, P., Jamonneau, V., Simarro, P. P., Ebeja, A. K., Sankara, D., & Dagne, D. A. (2023). Target product profile: diagnostic test for Trypanosoma brucei gambiense. *Bulletin of the World Health Organization*, *101*(8). https://doi.org/10.2471/BLT.23.290172

Qaiser, N., Khan, S. M., Babatain, W., Nour, M., Joharji, L., Shaikh, S. F., Elatab, N., & Hussain, M. M. (2023). A thermal microfluidic actuator based on a novel microheater. *Journal of Micromechanics and Microengineering*, *33*(3). https://doi.org/10.1088/1361-6439/acb4a3

Roberts, A., Chouhan, R. S., Shahdeo, D., Shrikrishna, N. S., Kesarwani, V., Horvat, M., & Gandhi, S. (2021). A Recent Update on Advanced Molecular Diagnostic Techniques for COVID-19 Pandemic: An Overview. In *Frontiers in Immunology* (Vol. 12). https://doi.org/10.3389/fimmu.2021.732756

Sharma, V., Koivikko, A., Yiannacou, K., Lahtonen, K., & Sariola, V. (2020). Flexible Biodegradable Transparent Heaters Based on Fractal-Like Leaf Skeletons. *NPJ Flexible Electronics*, *4*(1). https://doi.org/10.1038/s41528-020-00091-8

Solangi, N. H., Karri, R. R., Mubarak, N. M., & Mazari, S. A. (2024). Mechanism of polymer composite-based nanomaterial for biomedical applications. In *Advanced Industrial and Engineering Polymer Research* (Vol. 7, Issue 1). https://doi.org/10.1016/j.aiepr.2023.09.002

Sun, Q., Lu, Y., Xu, X., Huang, F., & Tang, C. (2018). Morphological Evolution and Migration Behavior of Silver Thin Films on Flexible Substrates During Thermal Cycle Testing. *Advances in Mechanical Engineering*, *10*(8), 168781401879596. https://doi.org/10.1177/1687814018795961

Tian, C., Li, Y., Wang, Y., Hu, X., Liu, L., & Shi, Y. (2023). Effect of Polyethylene Internal Structure on Antibacterial Properties of Nanosilver Composites. *Journal of Applied Polymer Science*, *140*(14). https://doi.org/10.1002/app.53706

Wang, H., Wang, M., Lei, W., Chen, X., Huang, H., & Wang, J. (2019). Wafer-level fabrication of low power consumption integrated alcohol microsensor. *Micro and Nano Letters*, *14*(1). https://doi.org/10.1049/mnl.2018.5183

Whulanza, Y., Ammar, H., Haryadi, D., Pangesty, A. I., Widoretno, W., Subekti, D. T., & Charmet, J. (2024). High-Performance, Easy-to-Fabricate, Nanocomposite Heater for Life Sciences and Biomedical Applications. *Polymers*, *16*(8). https://doi.org/10.3390/polym16081164

Whulanza, Y., Nathani, R. C., Adimillenva, K., Irwansyah, R., Wahyu Nurhayati, R., Utomo, M. S., & Abdullah, A. H. (2023). Effect of Flow Rate Modulation on Alginate Emulsification in Multistage Microfluidics. *Micromachines*, *14*(10). https://doi.org/10.3390/mi14101828

Whulanza, Y., Widyaratih, D. S., Istiyanto, J., & Kiswanto, G. (2014). Realization and testing of lab-on-chip for human lung replication. *ARPN Journal of Engineering and Applied Sciences*, *9*(11).

Yan, S., Zhu, X., Frandsen, L. H., Xiao, S., Mortensen, N. A., Dong, J., & Ding, Y. (2017). Slow-light-enhanced energy efficiency of graphene microheaters on silicon photonic crystal waveguides. *Nature Communications*, *8*. https://doi.org/10.1038/ncomms14411

Yang, J., Zi, D., Zhu, X., Li, H., Li, Z., Zhang, G., Wang, F., Peng, Z., & Lan, H. (2021). Printed Flexible Transparent Electrodes for Harsh Environments. *Advanced Materials Technologies*, *7*(5). https://doi.org/10.1002/admt.202101087

Zhang, N., Huang, C., Wan, S., Kang, L., Hu, M., Zhang, Y., Wu, X., & Zhang, J. (2019). A Novel Flexible Silver Heater Fabricated by a Solution-Based Polyimide Metalization and Inkjet-Printed Carbon Masking Technique. *ACS Applied Electronic Materials*, *1*(6). https://doi.org/10.1021/acsaelm.9b00109

Zhang, N., Huang, C., Wan, S., Lee, K., Hu, M., Zhang, Y., Wu, X., & Zhang, J. (2019). A Novel Flexible Silver Heater Fabricated by Solutiona Solution-Based Polyimide Metalization and Inkjet-Printed Carbon Masking Technique. *Acs Applied Electronic Materials*, *1*(6), 928–935. https://doi.org/10.1021/acsaelm.9b00109

Zhang, Q., Zou, J. X., Ai, J., Pan, X. T., Qiao, D. H., Jun, S. C., Jadhav, V. V., Kang, L., Huang, C., & Zhang, J. (2023). In Situ Construction of the Fe−Cu Hydroxide Interlocking Structure with Solution-Derived Cu/Ag Current Collectors for Flexible Symmetric Supercapacitors. *ACS Applied Materials and Interfaces*, *15*(47). https://doi.org/10.1021/ACSAMI.3C10925

Zhang, Y., Ren, G., Buss, J., Barry, A. J., Patton, G. C., & Tanner, N. A. (2020). Enhancing colorimetric loop-mediated isothermal amplification speed and sensitivity with guanidine chloride. *BioTechniques*, *69*(3). https://doi.org/10.2144/btn-2020-0078

Declaration of Competing Interest

The authors declare that they have no known competing financial interests or personal relationships that could have appeared to influence the work reported in this paper.